

# Non-Classical Smoothing of Nano-Scale Surface Corrugations

Jonah Erlebacher, Michael J. Aziz

*Harvard University, Division of Engineering and Applied Sciences, Cambridge, MA*

Eric Chason

*Brown University, Providence, RI*

Michael B. Sinclair, Jerrold A. Floro

*Sandia National Laboratories, Albuquerque, NM*

## Abstract

We report the first experimental observation of non-classical morphological equilibration of a corrugated crystalline surface. Periodic rippled structures with wavelengths of 290 – 550 nm were made on Si(001) by sputter rippling and then annealed at 650 – 750 °C. In contrast to the classical exponential decay with time, the ripple amplitude,  $A_\lambda(t)$ , followed an inverse linear decay,  $A_\lambda(t) = A_\lambda(0)/(1 + k_\lambda t)$ , agreeing with a prediction of Ozdemir and Zangwill. We measure the activation energy for surface relaxation to be  $1.6 \pm 0.2$  eV, consistent with an interpretation that dimers mediate transport.

## **DISCLAIMER**

**Portions of this document may be illegible in electronic image products. Images are produced from the best available original document.**

Mass transport during morphological equilibration of solid surfaces can occur through surface or bulk diffusion, viscous flow, or evaporation/recondensation. The dependence of the relaxation rate on temperature and feature size are related to basic surface energy parameters, both kinetic (e.g., surface diffusivity) and thermodynamic (e.g., surface tension). The theory of continuum surface relaxation, due primarily to Mullins [1] and Herring [2], and subsequent surface annealing experiments of sinusoidally grooved surfaces supporting this theory, notably by Blakely and co-workers [3], are considered classic studies in the materials science of surfaces. However, for the specific case of a crystalline surface that is near a singular orientation and below its thermodynamic roughening transition temperature,  $T_R$ , the classical theory is inapplicable [4, 5, 6, 7]. As a result, the amplitude of a shallow sinusoidal profile whose average orientation is a crystal facet is not necessarily expected to exhibit the classical exponential decay with time [8, 9, 10].

In this Letter, we report the first experimental observation of non-classical annealing behavior for a corrugated surface evolving toward planarity. We studied nanometer-scale ripples on Si(001) and observed a non-exponential decay for the time evolution of the ripple amplitude during anneals over the temperature range 650 - 750 °C. There have been several experimental approaches to morphological relaxation [11, 12, 13]. Our work is most similar to an earlier one by Keeffe, Umbach, and Blakely (KUB) [13], who studied the annealing behavior of Si(001) at higher temperatures (800 - 1100 °C) using lithographic techniques to produce sinusoidal patterns with larger wavelengths (4 - 6  $\mu\text{m}$ ) and amplitudes ( $\sim 100$  nm) than ours. In contrast to our results, however, KUB did observe exponential amplitude decay.

The nano-rippled samples used in these annealing experiments were produced by spontaneous pattern formation during low energy (500-1000 eV)  $\text{Ar}^+$  ion bombardment at glancing angles and elevated temperatures (“sputter rippling”) [14]. We used sputter rippling to produce rippled Si(001) samples (*p*-type, 3-10  $\Omega\text{-cm}$ , miscut  $0.1^\circ \pm 0.1^\circ$ ) for use in the surface relaxation experiments discussed here. Ripples ranged in wavelength from 290 - 550 nm, and in initial amplitude from 4 to 30 nm. The wavevectors of the ripples were oriented perpendicular to the [110] direction. Sample fabrication by sputter rippling in this kind of experiment is advantageous because the sample stays clean and

ripples can be made very small. Samples never see any *ex situ* lithographic or other kinds of preparation after the commencement of ion beam erosion, and many microns of material over a wide area ( $\sim 1 \text{ cm}^2$ ) are sputtered off in a clean ultra-high vacuum environment [15].

Morphological evolution during annealing was monitored using a recently developed *in situ* UV spectroscopic technique (“Light Scattering Spectroscopy”, LiSSp) that measures the spectrum of light scattered in a fixed direction [16]. Surface morphology information is contained in the measured intensity spectrum of the scattered light normalized by the incident light spectrum. This spectrum is proportional to the power spectral density (PSD) of the sample surface (the square of the magnitude of the Fourier transform of the surface profile, or equivalently, the surface height-height autocorrelation function). The intensity of the PSD at a particular spatial frequency is proportional to the square of the real amplitude of the surface measured at that spatial frequency. The constant of proportionality was found using *ex situ* atomic force microscopy (AFM) allowing absolute amplitude vs. time curves to be plotted. Details of our implementation of LiSSp, as well as sample spectral evolution, can be found in Ref. [17].

Fig. 1 shows AFM micrographs representative of the observed morphological evolution. Both samples shown in the figure had the same wavelength; however, the sample in Fig. 1A was not annealed while the one shown in Fig. 1B was annealed for a prolonged period of time. Figure 2 illustrates our key result – the ripple amplitude does not decay in the classical exponential manner at any time. Instead, for a ripple with wavelength  $\lambda$ , the time evolution of the amplitude,  $A_\lambda(t)$ , for all cases followed the inverse linear form

$$A_\lambda(t) = A_\lambda(0)/(1 + k_\lambda t). \quad (1)$$

The parameter  $k_\lambda$  contains all the temperature and scale dependence. The form of Eq. (1) is that of a non-classical model for the amplitude decay of perfect sinusoids presented by Ozdemir and Zangwill (OZ) [4] who built on earlier work by Rettori and Villain (RV)

[5] (we herein collectively refer to this model as RV-OZ). The salient points of the RV-OZ model are summarized as follows.

Consider a one-dimensional model for a decaying sinusoidal profile. In general, the local change in height  $h(x, t)$  at a point  $x$  on a surface is proportional to the divergence in the local flux of diffusing species  $j(x, t)$  at that point, a result simply due to mass conservation. That is,

$$\partial h(x, t)/\partial t \propto -\nabla \cdot j(x, t). \quad (2)$$

The local flux of the diffusing species on a surface during relaxation depends on the width of the terrace upon which the adatoms sit,  $l(x)$ , and also the local chemical potential difference between atoms on the steps bounding that terrace,  $\Delta\mu_0(x)$ . When the mass transport rate is limited by diffusion across the terrace,

$$j = (D_s C_0 / k_B T) \Delta\mu_0 / l, \quad (3)$$

where  $D_s$  is the surface diffusivity and  $C_0$  is the equilibrium concentration of adatoms on an infinitely wide terrace [18]. When the rate is limited by step traversal,

$$j = (a k_p C_0 / k_B T) \Delta\mu_0, \quad (4)$$

where  $k_p$  is the rate constant for hopping down a step onto the next lowest terrace [19] and  $a$  is the in-plane lattice constant. The connection between the continuum and the discrete is through the approximation that  $l(x) \propto 1/|\partial h(x)/\partial x|$ . With this approximation and the appropriate form for  $\Delta\mu_0$  (discussed below), a sinusoid with amplitude evolution given by Eq. (1) is found to be an approximate solution of Eq. (2) using either Eqs. (3) or (4) [4].

How the time-dependent behavior of the amplitude of a surface feature is related to a characteristic length scale of the overall surface morphology has been the subject of most theoretical studies of surface relaxation. RV-OZ show that the time decay of the amplitude of the infinite sinusoid obeys the following scaling behavior, derivable from careful consideration of the discrete forms the surface diffusive flux. In general, the amplitude  $A_\lambda(t)$  of a sinusoid with wavelength  $\lambda$  can be expressed as a universal amplitude decay function,

$$A_\lambda(t) = A(t/\lambda^n), \quad (5)$$

such as Eq. (1). The value of the scaling exponent,  $n$ , depends on the microscopic surface kinetics; for diffusion-limited kinetics (Eq. (3)),  $n = 5$ , and for step traversal-limited kinetics (Eq. (4)),  $n = 4$ . In the classical model, only diffusion limited kinetics are applicable and  $A(t/\lambda^n)$  is a decaying exponential with  $n = 4$ .

To find the full temperature dependence of Eq. (1), the form of  $\Delta\mu_0$  first needs to be clarified. Classically and above  $T_R$ , the chemical potential gradient is connected to the local morphology by a Gibbs-Thomson effect. In this case,  $\Delta\mu_0$  is proportional to the local curvature  $\kappa$  and the local surface energy,  $\gamma$ . Instead of continuum surface tension as a driving force for surface area reduction, the forces that drive relaxation are primarily due to step-step interactions. For discrete surfaces, the chemical potential of an atom at a step is proportional to the difference in the inverse cubes of the neighboring terrace lengths, a form expected when steps communicate only through elastic or entropic interactions [4, 5]. The constant of proportionality, typically written  $G_3(T)$ , describes the temperature dependence of the step-step interactions. If steps interact elastically then  $G_3$  is temperature independent; if the steps repel each other entropically then to first order,  $G_3 \propto (k_B T)^2$  [9]. It follows that  $\Delta\mu_0(x)$  in Eqs. (3), (4) has the temperature dependence of  $G_3$ .

The full temperature dependence of  $j(x)$  is found by multiplying the temperature dependence of  $\Delta\mu_0(x)$  by that of  $D_S$  or  $k_p$  and that of  $C_0$ . The latter three quantities are all thermally activated. Thus, we can write either product,  $D_S C_0$  or  $k_p C_0$  in a form proportional to  $\exp(-\varepsilon/k_B T)$ , where  $\varepsilon$  is an activation energy associated with the relaxation process. For diffusion-limited kinetics,  $\varepsilon = E_M + E_F$ . The migration energy  $E_M$  appears because the diffusivity  $D_S$  is thermally activated; the formation energy  $E_F$  appears because the equilibrium concentration of mobile species  $C_0$  is also thermally activated. For step traversal-limited kinetics,  $\varepsilon = E_p + E_F$ , where  $E_p$  is the step traversal barrier. Combining the temperature dependencies of  $D_S$ ,  $k_p$ , and  $C_0$  with that of  $G_3$  leads to the following temperature dependence for  $j(x)$ :

$$j(x) \propto \exp(-\varepsilon/k_B T) (k_B T)^m, \quad (6)$$

with  $m = \pm 1$ .

Equations (1), (2), (5), (6) can be combined so as to conclude that the full temperature and wavelength scaling dependencies of  $k_\lambda$  are of the form

$k_\lambda \propto \exp(-\varepsilon/k_B T) (k_B T)^m \lambda^{-n}$ . In fact, assuming the wavelength scaling behavior of Eq. (5), the particular form of  $A_\lambda(t)$  need not be known in order to find an activation energy for relaxation. The following data collapse strategy should be all that is required; it is essentially a three-parameter fit. Look for the best overlap of the amplitude relaxation curves,  $A_\lambda(t)$  vs.  $t \exp(-\varepsilon/k_B T) (k_B T)^m \lambda^{-n}$ , while varying the constrained set of parameters  $\{\varepsilon; m = \pm 1; n = 4, 5\}$ . The activation energy,  $\varepsilon$ , gives the sum of the formation energy and the rate limiting barrier to transport. The step-step interaction exponent,  $m$ , tells us whether steps interact entropically ( $m = -1$ ) or elastically ( $m = 1$ ). The scaling exponent tells us whether relaxation kinetics are diffusion-limited ( $n = 5$ ) or step traversal-limited ( $n = 4$ ).

Fig. 3 shows the best data collapses of the amplitude decay for all samples annealed between 650 and 750 °C. We find a slight preference for step traversal-limited kinetics ( $n = 4$ ) but we cannot distinguish entropic ( $m = -1$ ) and elastic interactions ( $m = +1$ ). In Fig. 3, data collapse for  $m = -1$  is shown, for which the best collapse is obtained for  $\varepsilon = 1.7$  eV. The only effect of replacing  $m = -1$  with  $m = +1$  for both  $n = 4$  or  $n = 5$  is that we obtain just as good a fit but with the value of  $\varepsilon$  reduced by 0.2 eV. Based on these results, we ascribe an activation energy of  $\varepsilon = 1.6 \pm 0.2$  eV with  $n = 4$  or 5 to the relaxation mechanism on Si(001) in this temperature range.

As discussed, one interprets the activation energy found in this type of experiment as a sum of the creation energy of the mobile surface species and the rate limiting barrier to transport. “Hot” and “atom tracking” STM measurements have found that the migration energy of dimers on Si(001) is  $E_M = 1.1 \pm 0.1$  eV [20]. Our own set of sputter induced rippling experiments suggests that in this temperature regime dimers are in fact the predominant species effecting transport and we measured a migration energy of  $E_M = 1.2 \pm 0.1$  eV [14]. Recently, Tromp et al. measured the formation energy of dimers on the Si(001) surface at temperatures in the range 750 to 1050 °C, and found that  $E_F = 0.35 \pm 0.05$  eV [21, 22]. As our results do not unequivocally distinguish between diffusion-limited and step traversal-limited kinetics, let us consider both possibilities. If transport is diffusion-limited then our best fit activation energy is 1.7 eV which we interpret as  $E_F + E_M$ . The independently-measured values of  $E_F$  and  $E_M$  sum to about 1.5 eV, which is within experimental error of our value. If transport is step traversal-limited then our best-fit activation energy is 1.6 eV which we interpret as  $E_F + E_P$ . The proximity of this value to the sum of the independently-measured values of  $E_F$  and  $E_M$  would then suggest that the barriers for step traversal and terrace migration in this system are similar [23].

The RV-OZ model of surface relaxation is applicable to perfect sinusoidal surfaces with no crossing steps. Despite the obvious irregularities on our sputter rippled surfaces, we find it works well to describe the annealing behavior. It has been suggested that “crossing steps,” at the extrema of the terraces, play an important role during annealing of Si(001) [24]. One can in fact construct a rippled surface comprised entirely of very high

amplitude crossing steps. The direction of the ripple wavevector,  $[1\bar{1}0]$ , and the small miscut of our samples,  $0.1^\circ \pm 0.1^\circ$ , are such that our ripples should be comprised of alternating  $S_A$  and  $S_B$  steps running along  $[110]$  with relatively few steps crossing adjacent peaks and valleys. The sides of the ripples should have steps of opposite sign, fulfilling the basic morphological requirement of the RV-OZ model. We note, however, that the RV-OZ model neglects step-step interactions at the uppermost and lowermost terraces as well as the overall reduction in surface energy when steps are annihilated. It may be that these effects are simply not important for this material system under our experimental conditions.

To conclude, we find that the decay behavior of clean, rippled patterns does not follow the classical exponential decay time dependence of Mullins and Herring. Instead, an inverse linear decay is observed, consistent with the RV-OZ model. The activation energy for relaxation at  $650 < T < 750$  °C,  $1.6 \pm 0.2$  eV, is close to the sum of the dimer migration and formation energies measured independently.

The authors acknowledge stimulating discussions with E. Kaxiras, D. Kandel, J. Sethna, D. G. Cahill and M.V.R. Murty and technical advice given by John Hunter. This work was supported by DE-FG08-89ER45401. Portions of this work were performed at Sandia National Laboratories, supported by the United States Department of Energy under contract DE-AC04-94AL85000.

## References

- [1] W.W. Mullins, *J. Appl. Phys.* **28** (1957), 333; W.W. Mullins, *J. Appl. Phys.* **30** (1959), 77
- [2] C. Herring, in: *Structure and Property of Solid Surfaces*, Eds. R. Gomer and C.S. Smith (University of Chicago Press, 1953), p. 5.
- [3] J.M. Blakely and H. Mykura, *Acta Met.* **10** (1962), 565; P.S. Maiya and J.M. Blakely, *J. Appl. Phys.* **38** (1967), 698.
- [4] M. Ozdemir and A. Zangwill, *Phys. Rev. B* **42** (1990), 5013.
- [5] A. Rettori and J. Villain, *J. Phys. France* **49** (1988), 257.
- [6] H. P. Bonzel and W.W. Mullins, *Surf. Sci.* **350** (1996), 285; F. Lancon and J. Villain, *Phys. Rev. Lett.* **64** (1990), 293; W. Selke and P.M. Duxbury, *Phys. Rev. B* **52** (1995), 17468; H.P. Bonzel and E. Preuss, *Surf. Sci.* **336** (1995), 209.
- [7] P. Nozieres, *J. Physique*, **48** (1987), 1605.
- [8] Z. Jiang and C. Ebner, *Phys. Rev. B* **40** (1989), 316; Z. Jiang and C. Ebner, *Phys. Rev. B* **53** (1996), 11146.
- [9] J. D. Erlebacher, M. J. Aziz., *Surf. Sci.*, 374 (1997), 427; J. D. Erlebacher, in *Dynamics of Crystal Surfaces and Interfaces*, Eds. P.M. Duxbury and T.J. Pence. (Plenum Press, New York, 1997), 97.
- [10] Under certain special circumstances, exponential decay can be expected below  $T_R$ , as discussed by M. Uwaha, *J. Phys. Soc. Japan*, **57**, (1988), 1681; S. J. Chey, D. G. Cahill, , in *Dynamics of Crystal Surfaces and Interfaces*, Eds. P.M. Duxbury and T.J. Pence. (Plenum Press, New York, 1997), 59.
- [11] S. Tanaka, N.C. Bartelt, C. C. Umbach, R.M. Tromp, J.M. Blakely, *Phys. Rev. Lett.* **78** (1997), 3342.
- [12] S.J. Chey, J.E. Van Nostrand, D.G. Cahill, *Phys. Rev. Lett.* **76** (1996), 3995.
- [13] M.E. Keeffe, C.C. Umbach, J.M. Blakely, *J. Phys. Chem. Solids* **55** (1994), 965.
- [14] J. Erlebacher, M.J. Aziz, E. Chason, M.B. Sinclair, J.A. Floro, *Phys. Rev. Lett.*, **82** (1999), 2330.
- [15] The chamber base pressure was  $2.0 \times 10^{-10}$  Torr. We do not believe that a background contamination of the surface due to the presence of residual gases in the

chamber is poisoning the relaxation over long time scales, because we see the same non-exponential decay behavior for experiments at high temperature lasting only a few tens to hundreds of seconds as for experiments at low temperatures lasting many thousands of seconds.

- [16] E. Chason, M. B. Sinclair, J. A. Floro, J. A. Hunter, R. Q. Hwang, *Appl. Phys. Lett.* **72**, 3276 (1998).
- [17] J. Erlebacher, M.J. Aziz, E. Chason, M.B. Sinclair, J.A. Floro, in preparation.
- [18] Note that Eq. (3) contains an implicit assumption of being near equilibrium – it allows  $C_0$  to be written in a thermally activated form.
- [19] For Si(001) there appears to be two pathways for step traversal. One is the conventional attachment and detachment from the step edge. The other is direct permeation without attachment, as discussed in [9]. Whichever has the lower barrier will be relevant for Eq. (4).
- [20] M. Krueger, B. Borovsky, E. Ganz, *Surf. Sci.* **385** (1997), 146. B. S. Swartzentruber, *Phys. Rev. Lett.* **76** (1996), 459. B. S. Swartzentruber, A. P. Smith, H. Johnson, *Phys. Rev. Lett.* **77** (1996), 2518.
- [21] R.M. Tromp and M. Mankos, *Phys. Rev. Lett.* **81** (1998), 1050.
- [22] N.C. Bartelt, W. Theis, R.M. Tromp, *Phys. Rev. B*, **54** (1996), 11741; W. Theis, N.C. Bartelt, R.M. Tromp, *Phys. Rev. Lett.* **75** (1995), 3328.
- [23] The apparent activation energy for the step-mobility, a related phenomenon, was estimated to be 1.8 eV by Chey and Cahill (Ref. [10]) by interpreting a variety of experiments.
- [24] C.C. Umbach, M.E. Keeffe, J.M. Blakely, *J. Vac. Sci. Tech. A* **11** (1993), 1830.

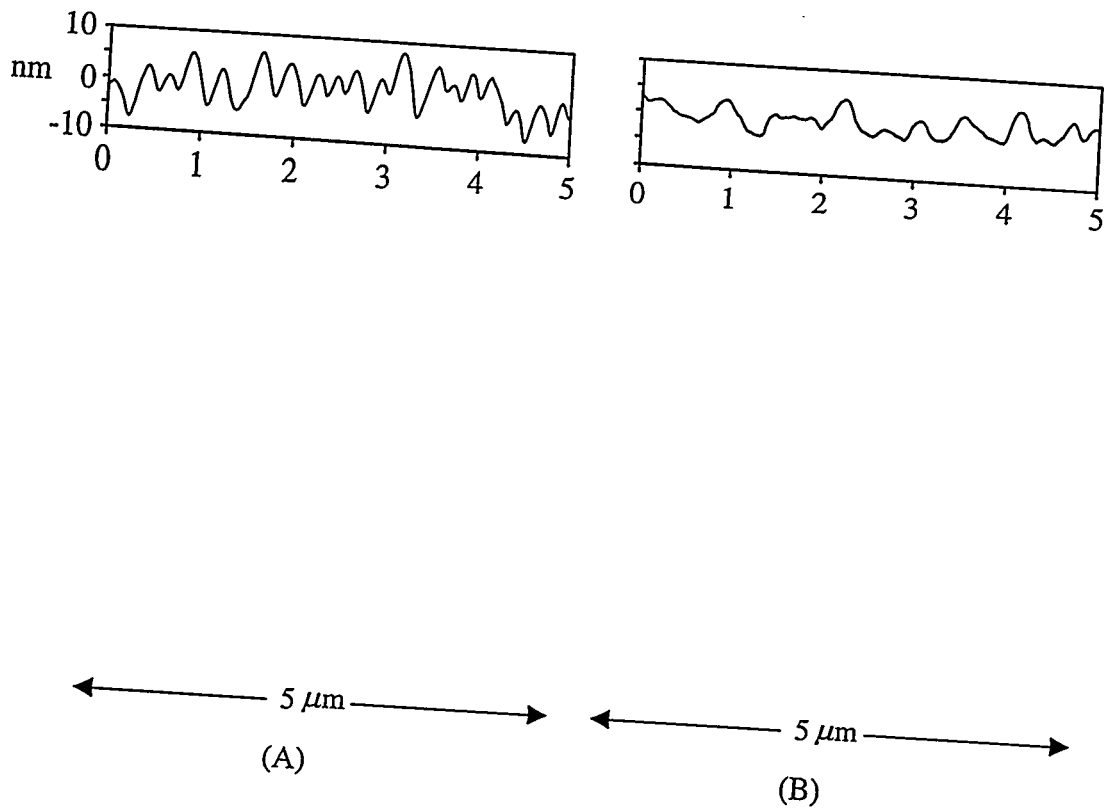


Figure 1. Example AFM micrographs of (A) an unannealed rippled sample,  $\lambda = 360$  nm and (B) a post-annealed sample,  $\lambda = 363$  nm,  $T_{\text{anneal}} = 667$  °C, annealing time = 2145 sec. The representative line scans for each micrograph are the horizontal centerlines. The gray scales are the same for each image.

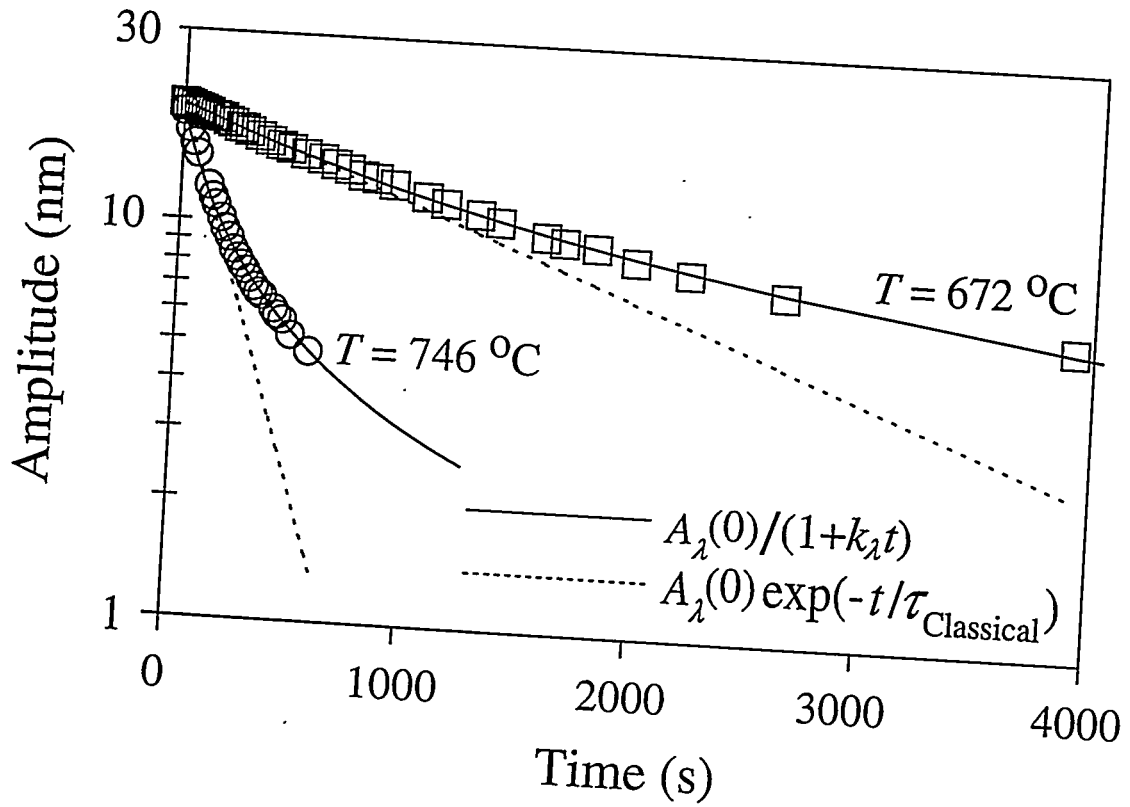


Figure 2. Typical amplitude decay behavior (data: squares, circles) during an *in situ* anneal, illustrating the non-classical decay behavior (classical: dashed lines) and the good fit to the RV-OZ form, Eq. (1) (solid lines). For these samples,  $\lambda = 565\text{ nm}$ ,  $T = 672\text{ }^{\circ}\text{C}$  (squares),  $\lambda = 485\text{ nm}$ ,  $T = 746\text{ }^{\circ}\text{C}$  (circles).

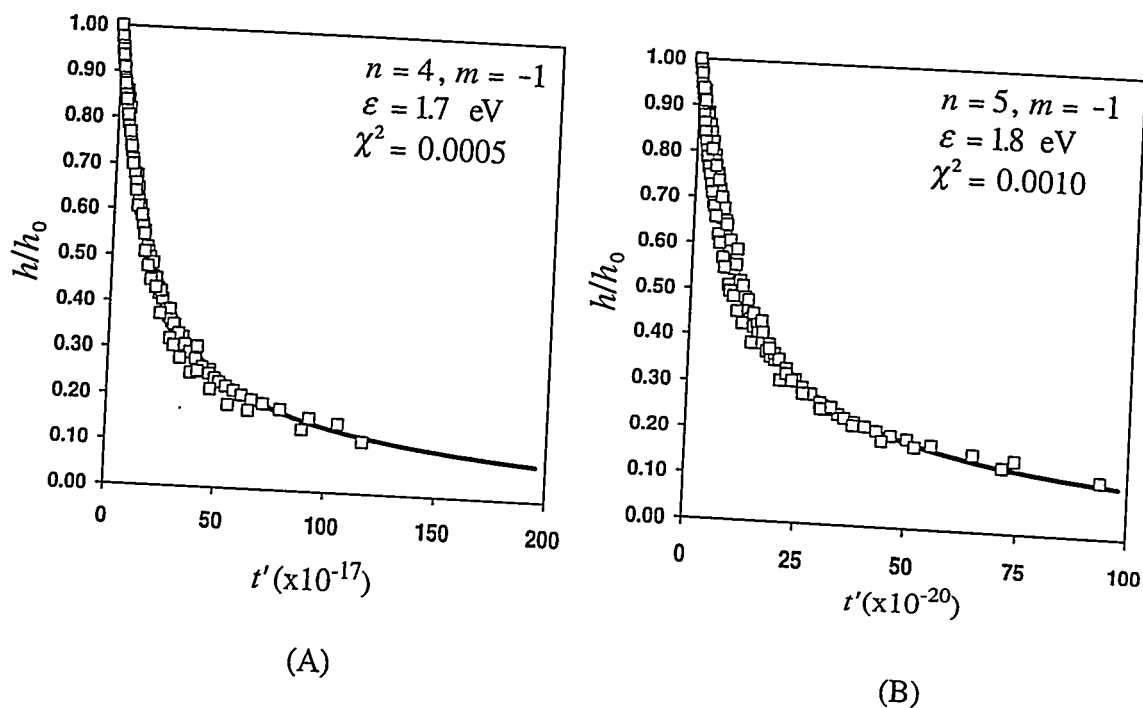


Figure 3. Best Data Collapses for relaxation data assuming step traversal-limited kinetics (A:  $n=4$ ) and diffusion-limited kinetics (B:  $n=5$ ). The scaled time,  $t' = t(k_B T)^m \exp(-\varepsilon/k_B T) \lambda^{-n}$ , as discussed in the text. Data are shown as open squares. The best fit to Eq. (1) is shown as a solid line and the associated  $\chi^2$  deviations from the data collapse are reported.